address with the combination of these behavioral methods and population-based neurophysiology.

References and Notes

1. K. Lashley, in *Cerebral Mechanisms in Behavior*, L. A. Jeffress, Ed. (Wiley, New York, 1951), pp. 112–136.
2. R. Held, S. J. Freedman, *Science* **142**, 455 (1963).
3. C. Harris, *Psychol. Rev*. **72**, 419 (1965).
4. Two groups of human subjects performed the drawing tasks. In the first group, subjects described their perception of the drawings verbally and those in the second set reported by drawing the last cycle of the task in the dark. Both groups reported (incorrectly) that they had drawn an oval in the fifth circuit of the illusion task (SOM text, "Human reports").
5. J. H. Lee, P. van Donkelaar, abstract presented at the 31st Annual Meeting of the Society for Neuroscience, San Diego, CA, 10 to 15 November 2001.
6. D. M. Clower *et al.*, *Nature* **383**, 618 (1996).
7. K. Kurata, E. Hoshi, *J. Neurophysiol.* **81**, 1927 (1999).
8. A. P. Georgopoulos, R. E. Kettner, A. B. Schwartz, *J. Neurosci.* **8**, 2928 (1988).
9. A. B. Schwartz, *Science* **265**, 540 (1994).
10. D. W. Moran, A. B. Schwartz, *J. Neurophysiol.* **82**, 2676 (1999).
11. E. V. Evarts, *J. Neurophysiol*. **31**, 14 (1968).
12. J. F. Kalaska, D. A. D. Cohen, M. L. Hyde, M. Prud'homme, *J. Neurosci*. **9**, 2080 (1989).
13. G. A. Reina, D. W. Moran, A. B. Schwartz, *J. Neurophysiol*. **85**, 2576 (2001).
14. J. Ashe, A. P. Georgopoulos, *Cereb. Cortex* **6**, 590 (1994).
15. Q.-G. Fu, D. Flament, J. D. Coltz, T. J. Ebner, *J. Neurophysiol.* **73**, 836 (1995).
16. A. P. Georgopoulos, J. T. Lurito, M. Petrides, A. B. Schwartz, J. T. Massey, *Science* **243**, 234 (1989).
17. A. F. Carpenter, A. P. Georgopoulos, G. Pellizzer, *Science* **283**, 1752 (1999).
18. M. V. Chafee, D. A. Crowe, B. B. Averback, A. P. Georgopoulos, abstract presented at the 30th Annual Meeting of the Society for Neuroscience, New Orleans, LA, 4 to 9 November 2000.
19. J. E. Lateiner, R. L. Sainburg, *Exp. Brain Res*. **151**, 446 (2003).
20. D. Pelisson, D. Prablanc, M.A. Goodale, M. Jennerod, *Exp. Brain Res.* **62**, 303 (1986).
21. Materials and methods are available as supporting material on *Science* Online.
22. Eccentricity was calculated as a ratio of the horizontal to vertical amplitude of each ellipse. A nonlinear algorithm was used to fit the sinusoidal components of the ellipse separately in each dimension.
23. G. A. Reina, A. B. Schwartz, *Hum. Mov. Sci.* **22**, 137 (2003).
24. M. A. Lebedev, S. P. Wise, *Behav. Cog. Neurosci. Rev.* **1**, 108 (2002).
25. S. T. Carmichael, J. L. Price, *J. Comp. Neurol.* **363**, 642 (1995).
26. M.-T. Lu, J. B. Preston, P. L. Strick, *J. Comp. Neurol.* **341**, 375 (1994)
27. L. G. Ungerleider, M. L. Mishkin in *Analysis of Visual Behavior*, D. J. Ingle, M. A. Goodale, R. J. W. Mansfield, Eds. (MIT Press, Cambridge, MA, 1982), pp. 549–586.
28. B. B. Averbeck, M. V. Chafee, D. A. Crowe, A. P. Georgopoulos, *Proc. Natl. Acad. Sci. U.S.A.* **99**, 13172 (2002).
29. B. B. Averbeck, M. V. Chafee, D. A. Crowe, A. P. Georgopoulos, *Exp. Brain Res*. **150**, 127 (2003).

30. Supported by NIH (R01 NS26375), the Neurosciences Research Foundation and the University of Pittsburgh School of Medicine. M. Velliste and A. Harris developed and performed the human experiments. We thank E. Ycu for technical support, as well as J. Vega and A. Kakavand.

Supporting Online Material

www.sciencemag.org/cgi/content/full/303/5656/380/DC1
Materials and Methods
SOM Text
Figs. S1 to S6
Tables S1 and S2

9 June 2003; accepted 7 November 2003

RNA Leaching of Transcription Factors Disrupts Transcription in Myotonic Dystrophy

A. Ebralidze, Y. Wang, V. Petkova, K. Ebralidse, R. P. Junghans*

Myotonic dystrophy type 1 (DM1) is caused by a CUG_n expansion ($n \approx 50$ to 5000) in the 3′ untranslated region of the mRNA of the DM protein kinase gene. We show that mutant RNA binds and sequesters transcription factors (TFs), with up to 90% depletion of selected TFs from active chromatin. Diverse genes are consequently reduced in expression, including the ion transporter CIC-1, which has been implicated in myotonia. When TF specificity protein 1 (Sp1) was overexpressed in DM1-affected cells, low levels of messenger RNA for CIC-1 were restored to normal. Transcription factor leaching from chromatin by mutant RNA provides a potentially unifying pathomechanistic explanation for this disease.

Myotonic dystrophy type 1 (DM1) is an autosomal dominant disorder linked to a monoallelic expansion of the CTG_n repeat in the 3′ untranslated region of the DM protein kinase gene (*DMPK*); healthy individuals have repeats of $n = 5$ to 37, whereas affected individuals have repeats of $n = 50$ to 5000 (*1*). The mechanism of DM1 pathogenesis and its multisystem presentation has spawned many hypotheses (*2*–*8*), but a satisfyingly unifying concept has yet to emerge.

We hypothesized that *DMPK* mutant RNA might exert its deleterious effects through a transcriptional mechanism by direct binding of basic transcription factors (TFs). Because mutant RNA is known not to transport to the cytoplasm but to coalesce into ribonucleoprotein (RNP) foci in the nucleus (*9*, *10*), this association had the potential to divert these factors from their essential transcriptional functions.

If TFs are selectively sequestered by mutant RNA in DM1-affected cells, it should be possible to show mutant RNA but not other RNAs in complex with the affected TFs in vivo (*11*). As a cell source, we applied the widely used model of *MyoD*-generated "myocytes" from normal and DM1 subjects, which leads to equivalent muscle-specific *DMPK* gene induction in control and mutant cells: Control cells express only wild-type *DMPK* mRNA; DM1 cells express both wild-type and mutant RNAs (*10*). DM1 cells (CTG_{100}) showed selective *DMPK* mutant RNA coprecipitation (dual bands; Fig. 1) with TFs Sp1 and retinoic acid receptor gamma (RARγ) and, as a positive control, CUG-binding protein 1 (CUGBP1), for its known affinity for mutant versus wild-type *DMPK* mRNA in vivo (*4*). α-Actin and β-actin mRNAs were not detectable in any of the complexes. In contrast, *DMPK* mutant RNA was not coprecipitated with nuclear pore proteins complex, nuclear pore component NUP153, or platelet-derived growth factor (PDGF) membrane receptor. With control cells, no *DMPK* wild-type mRNA (single band) was recovered bound to any of the proteins. Equivalent results were obtained with a second DM1 cell line, GM03132 (CTG_{2000}) (*12*). These data demonstrate that TFs are selectively complexed in vivo by mutant, but not by wild-type, *DMPK* mRNA or heterologous (α- or β-actin) mRNAs.

To address the core mechanistic element of this hypothesis, i.e., that TFs are depleted from their sites of action in mutant RNA–expressing cells, we examined whether mutant RNA binding of TFs correlated with a disturbance to their normal distribution among nuclear compartments. For TFs, we studied representatives of three classes, associated nominally with cell maintenance (Sp family, Sp1 and Sp3); activation (signal transducer and activator of transcription family, STAT1 and STAT3); and differentiation (RARγ). For 4 weeks after *MyoD* induction, control cells maintained their stable distribution, with RARγ residing mainly in chromatin instead of RNP (Fig. 2, A and B). In contrast, over the same period, DM1-affected cells showed a progressive decline in the ratio of TF in chromatin versus that in RNP, such that RNP became the dominant site. At 4.5 weeks, all four DM1-affected lines showed a similar, pronounced fivefold redistribution of RARγ toward the RNP (Fig. 2, C and D, top).

The four other TFs from the Sp and STAT families (Fig. 2D, bottom) were all nearly absent from RNP before mutant RNA induction, which precluded a derived baseline chromatin/RNP ratio (>10). After 3 weeks of

Biotherapeutics Development Lab, Harvard Institute of Human Genetics, Harvard Medical School and Division of Hematology-Oncology, Beth Israel Deaconess Medical Center, 4 Blackfan Circle, Boston, MA 02215, USA.

*To whom correspondence should be addressed. E-mail: junghans@hms.harvard.edu

mutant RNA expression, however, the measured fractions of TF in chromatin in the DM1 cells shifted dramatically for Sp1, STAT1, and STAT3, with levels of 30, 14, and 32%, respectively, versus ~100% in chromatin for control. Sp3 was only minimally affected; 75% of it remained in chromatin.

Did the "redistribution" ratio data in Fig. 2, A to D, represent an actual depletion from chromatin or merely an accumulation in the RNP and protection of unbound TF that would normally have been turned over? Chromatin isolations were repeated under conditions controlled for equivalent absolute numbers of viable myocytes. Stable levels of TF in chromatin were seen in normal cells at 4 weeks as compared with 0 weeks of *DMPK* expression, but a marked drop in DM1-affected cells was apparent over the same period (Fig. 2E). Two additional DM1 cell lines similarly showed markedly lower RARγ levels in chromatin after 4.5 weeks of mutant RNA expression (Fig. 2F). The net amount of RARγ remaining in chromatin was 9, 15, and 11% of control after mutant RNA induction. Hence, these tests demonstrate an authentic leaching of TFs out of the chromatin and into the RNP fraction that is specifically mediated in mutant RNA–expressing DM1 cells. However, these measured depletions of TF from chromatin are even more severe than the maximum changes of three- to fivefold expected from the redistribution model (Fig. 2C).

Loss of TFs from chromatin in DM1 means loss from their sites of action. We therefore examined whether gene expression was broadly affected in concert with the TF depletion. Whereas TFs are themselves dependent on TFs for their own transcription (*13*), the same TFs could also be subject to transcriptional depression. Northern blotting of cellular RNA 4.5 weeks after *DMPK* induction revealed the following: a moderate reduction of glyceraldehyde-3-phosphate dehydrogenase (*GAPDH*) mRNA (~35% decrease) in DM1 versus normal cells; no change in *FCGRT* (Fc IgG receptor for transport, Brambell receptor) mRNA (~5% increase) or in α-actin or β-actin mRNAs; and significantly lower mRNA levels for TFs *Sp1*, *Sp3*, and *RAR*γ (~50% reduction) and lesser reduction of *Sp2* (~20%) (Fig. 3A).

As corroboration, multiplex reverse transcription polymerase chain reaction (RT-PCR) was conducted to quantify RNA levels (Fig. 3B). Before *DMPK* expression (–MyoD), DM1 and control cells began with equal levels for all RNAs. After *DMPK* induction (+MyoD), changes were pronounced for *GAPDH*, *CLCN1*, *Sp1*, *Sp3*, and *RAR*γ, with average mRNA suppression in the four DM1 mutant RNA–expressing cell lines of −41, −70, −46, −50, and −44% relative to wild-type cells, respectively. No significant change was observed in *FCGRT*, α-actin, or β-actin gene expression or in 18*S* RNA (Fig. 3, B and C). All values were close to the corresponding numbers estimated by Northern blot phosphorescence imaging (Fig. 3A).

Hence, maldistribution (leaching) of TFs can lead to reduced expression of selected genes, including that of TFs themselves. When TF transcription is also reduced, it compounds the impact of mutant RNA leaching to deplete TFs from chromatin. This accords with our RARγ results that showed greater net suppressions of TF in chromatin (Fig. 2, E and F) than that predicted by redistribution alone (Fig. 2C). If mutant RNA–induced redistributions by factors of 2 to 5 and reductions in mRNA by of as much as a factor of 2 for selected TFs are considered nominal, then overall reductions by a factor of 5 to 10 (to 10 to 20% of normal) in chromatin may be commonplace among TFs in DM1 setting.

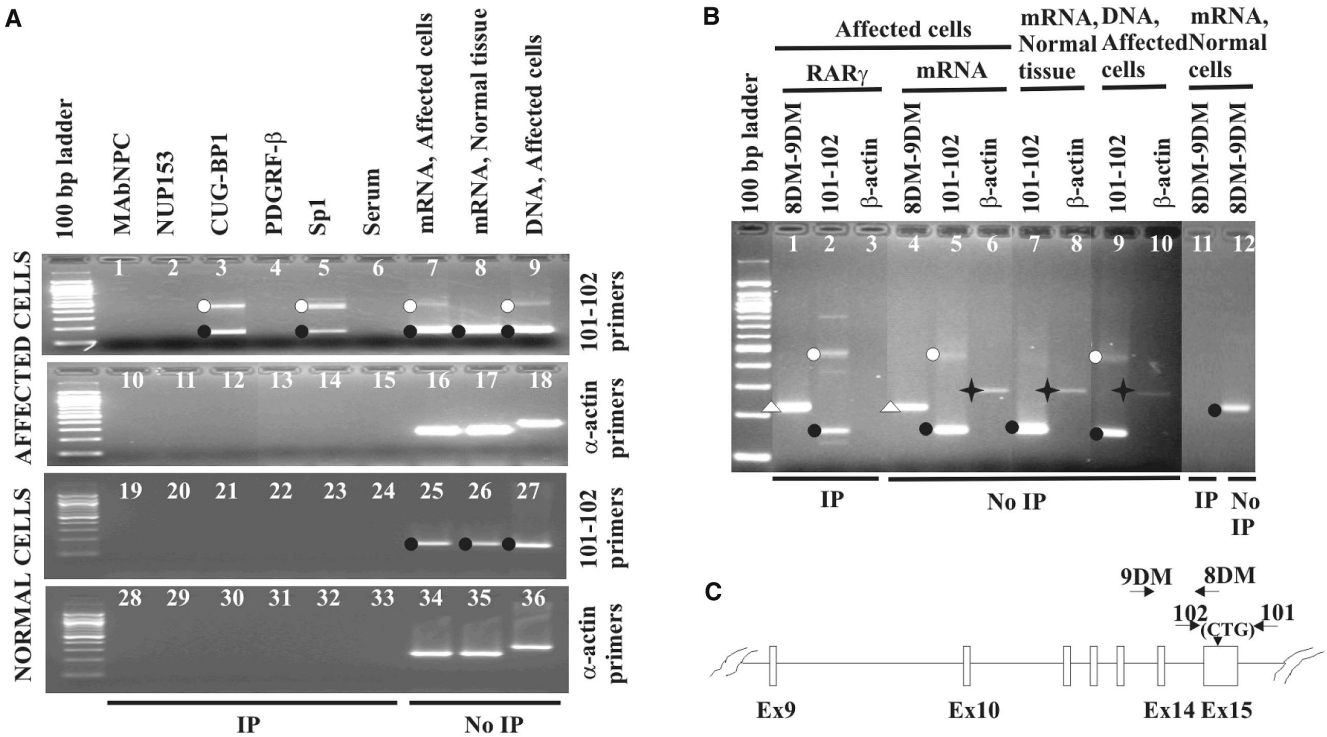

Fig. 1. Nuclear TFs selectively bind mutant mRNA in vivo. (**A**) Sp1. Nuclear extracts from DM1 and normal cells underwent PCR after immunoprecipitation ("IP") or not ("No IP"), per nRIP protocol (see Methods). *DMPK* mutant mRNA in precipitate revealed by dual bands. (**B**) RARγ. (**C**) Interpretation of bands. Primer pair 101-102 flanks CUG_n. Wild-type *DMPK* mRNA generates single band [150 nt (●)] and mutant *DMPK* mRNA dual bands [150 nt (●) and 450 nt (○)] of approximately equal intensity (150 > 450), with the smaller band arising by template sliding across expanded CUGn during PCR (*17*, *30*) (fig. S1). PCR efficiency is poorer for mutant than wild-type templates: equimolar mutant and wild-type *DMPK* in DM1 cellular DNA [lane 9 in (A)] shows strong dominance of low-molecular-mass PCR band (●) (150 ≫ 450), also evident in "No IP" DM1 mRNA [lane 7 in (A)]. Primer pair 8DM-9DM spans exons 14 to 15 with same size (△) and amplification efficiency for mutant and wild-type RNAs. Actin control [✦ in (B)] was not present in any IP.

We examined *CLCN1*, the gene encoding CIC-1, the skeletal muscle chloride channel whose disruption has been implicated in DM1 myotonia (*6*, *7*). The impact of DM1 on *CLCN1* mRNA levels in humans has been controversial (*7*, *14*). In muscle of long-repeat (CTG_{250}) transgenic mice, reductions by factors of 2.5 to 3 (to 31 to 43% of normal) were observed (*6*). Our own tests of *CLCN1* mRNA in DM1-affected cells showed suppression in transcript levels by factors of 3 to 6 across four cell lines (to 15 to 35% of normal) and support a common phenomenon in human and mouse models.

A search for TF binding motifs within the 300-nt *CLCN1* promoter region (*15*) revealed 18 sites with similarity higher than 0.7 for Sp1 consensus, in addition to the three putative E-box sites for TFs of the helix-loop-helix (HLH) family, class I: E47 and class II: MyoD, which bind as heterodimers (*16*). We confirmed (*17*) indicated the Sp1-binding activity of such sites and their structural compatibility for assembly into canonical transcription initiation complexes (supporting online materials; fig. S2). Because Sp1 is one of the TFs most affected by mutant RNA binding, Sp1 depletion could be a proximate cause of depressed *CLCN1* transcription in DM1-affected cells. Therefore, we tested whether "replenishment" of Sp1 in the same cells could reverse this finding.

Under conditions of induced *DMPK*, the GM0433 cell line displayed a factor of 3 depression (–68%) of *CLCN1* mRNA, to 32% of control. When these affected cells were transduced with a high-expressing Sp1 plasmid to restore Sp1 "sufficiency," the depressed *CLCN1* mRNA was increased 2.8-fold (+280%), which restored it to normal levels (Fig. 3, C and E). A nonspecific effect of Sp1 overexpression on all genes was ruled out by lack of impact on negative control gene *FCGRT* in the same cells, which was not depressed in DM1-affected cells. Overexpression of Sp3, the TF that was most resistant to mutant RNA–induced redistribution in vivo, had no effect on *CLCN1* or on *FCGRT* mRNA levels in mutant RNA–expressing cells. These data are compatible with an important role for Sp1 in *CLCN1* regulation and, correspondingly, support the potential of diverse TF depletions in DM1-affected cells to depress transcription of *CLCN1* and other genes in vivo.

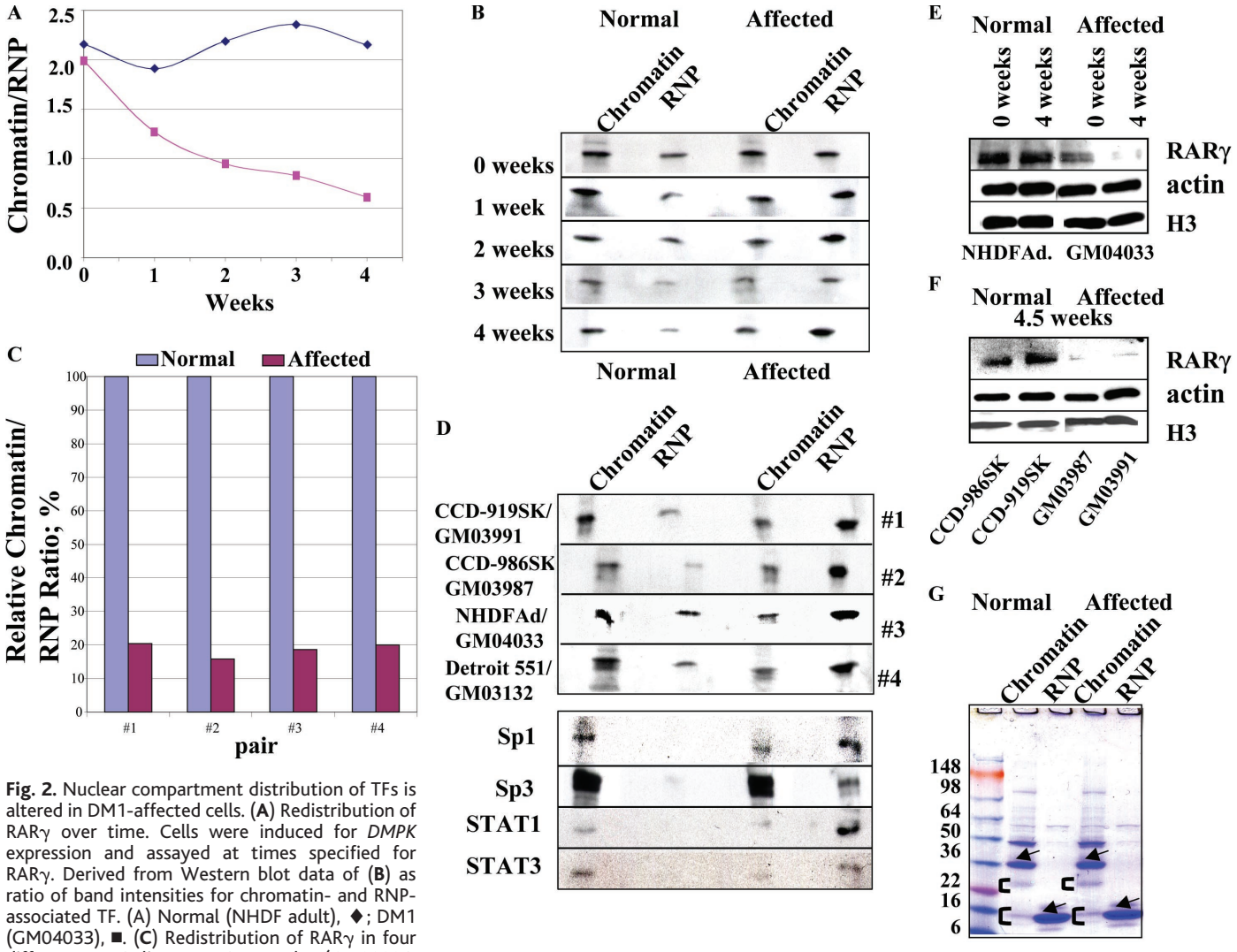

Fig. 2. Nuclear compartment distribution of TFs is altered in DM1-affected cells. (**A**) Redistribution of RARγ over time. Cells were induced for *DMPK* expression and assayed at times specified for RARγ. Derived from Western blot data of (**B**) as ratio of band intensities for chromatin- and RNP-associated TF. (A) Normal (NHDF adult), ◆; DM1 (GM04033), ■. (**C**) Redistribution of RARγ in four different DM1 lines at 4.5 weeks (GM03991, GM03987, GM04033, and GM03132). Derived from Western blot data of (**D**, top) as normalized chromatin/RNP RARγ ratio in DM1 versus normal counterpart's ratio, assigned as 100%. (D, bottom). Chromatin-RNP fractions for Sp- and STAT-family TFs at 3 weeks of culture. (**E**) Reduction of RARγ in DM1 chromatin during cultivation. Normal (NHDF adult), DM1 (GM04033). (**F**) At a fixed time (4.5 weeks), TF is lower in DM1 chromatin (GM03987 and GM03991) than in normal (CCD-986SK and CCD-919SK). (**G**) Chromatin and RNP loading. Coomassie staining of chromatin and RNP from normal (NHDF adult) and DM1 (GM04033). Top arrows, deoxyribonuclease I (DNase I) to solubilize chromatin samples; bottom arrows, ribonuclease (RNase) to solubilize RNP samples. Brackets mark histones H1 (top) and H3, H2B, H2A, and H4 (bottom). Equivalent histone bands prove uniformity of chromatin extractions.

CLCN1 mRNA has been shown in DM1 to exhibit an increase in aberrant splicing of pre-mRNA that serves to further depress levels of functional CIC-1 protein beyond that due to low total mRNA (*7*). Reduced total *CLCN1* mRNA levels were initially proposed to result from nonsense-mediated decay (NMD) to rapidly clear misspliced *CLCN1* transcripts (*6*, *7*), although a role for NMD was not directly demonstrated [e.g., in the manner of (*18*)]. In light of our data, it may alternately be suggested that low *CLCN1* mRNA levels in DM1 may derive from depressed *CLCN1* transcription as a dominant primary effect, on which splicing disruptions may secondarily be imposed.

Our results support the hypothesis that mutant RNA binds and sequesters nuclear TFs in DM1 myocytes and leads to disrupted gene expression patterns. This binding induces a redistribution of TFs away from active chromatin and toward an RNP fraction of the nuclear matrix for four out of five general transcription factors. Inasmuch as nuclear structural and cytoplasmic membrane proteins were not similarly bound by mutant RNA, the basis for this interaction between TF and mutant RNA appears to reside in the proteins' normal capacity for nucleic acid (double-stranded DNA) binding, possibly with analogous double-stranded regions in the mutant RNA itself (*19*). However, the TF–mutant RNA binding lacks particular sequence specificity that is the hallmark of the TF-DNA interactions.

We also show that maldistribution of TFs can lead to reduction in total TF transcription, the combined effects of which can be a net factor of 5 to 10 (80 to 90%) depletion of select chromatin-associated TFs. These data thus present a scenario with the potential for massive derangement of transcription in affected cells. Mutant RNA–induced leaching of TFs from chromatin led to significant (>30%) reductions in mRNA expression (*20*) in several of the genes examined. However, the disruption was not general: An equal number maintained normal or near-normal transcript

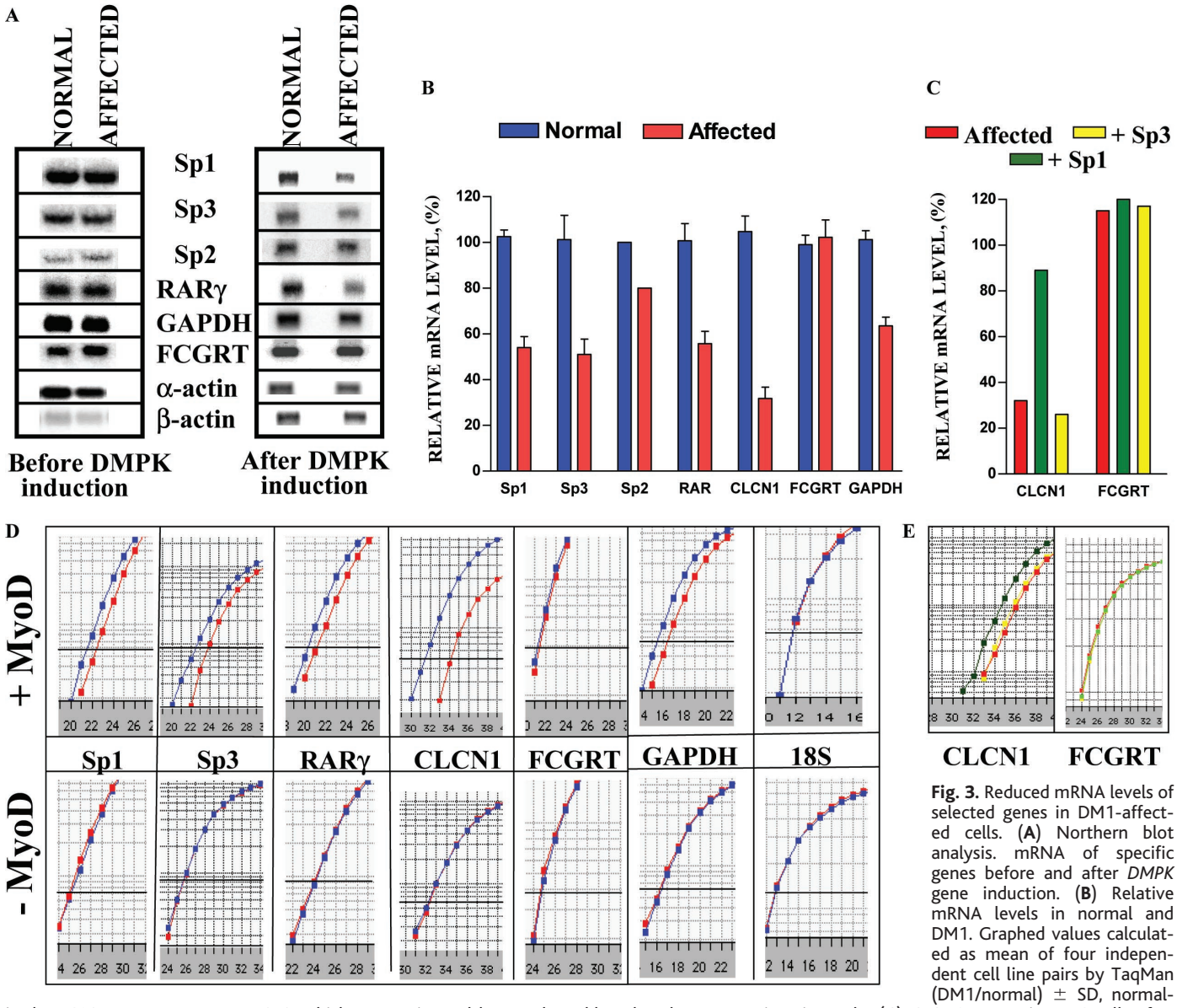

Fig. 3. Reduced mRNA levels of selected genes in DM1-affected cells. (**A**) Northern blot analysis. mRNA of specific genes before and after *DMPK* gene induction. (**B**) Relative mRNA levels in normal and DM1. Graphed values calculated as mean of four independent cell line pairs by TaqMan (DM1/normal) ± SD, normalized to 18*S* per extract, except *Sp2*, which was estimated by Northern blot phosphorescence imaging only. (**C**) *CLCN1* mRNA in DM1 cells after Sp-family overexpression. Baseline mRNA relative to paired normal was 32% for *CLCN1* and 115% for *FCGRT*. (**D**) TaqMan gene-specific amplification plots such as used for (B). (**E**) TaqMan analysis of mRNA in DM1-affected cells after Sp family overexpression. *MyoD*-transduced GM04033 cells at 4 weeks were untransfected or transfected with plasmids for Sp1 or Sp3, with elevated TF expressions by TaqMan (*12*). Changes in (E) are graphed relative to baseline (Affected) after Sp1 and Sp3 overexpression as shown in (C).

levels under the same conditions. With the addition of seven further genes recently examined (*21*), the fraction of genes with significantly reduced mRNA levels is 8/16 or 50% (95% confidence limits: 27 to 73%).

This effect on TFs in DM1 suggests comparisons with Huntington's disease (HD) in which huntingtin selectively binds and disrupts Sp1 (*22*, *23*). However, this protein-protein interaction in HD is more restricted than the RNA-protein interaction in DM1, which sequesters many TFs concurrently. Correspondingly, the extent of derangement of gene transcription in HD models (estimated at ~2%) (*24*) is far less than seen in our DM1 sample (50%).

A common requirement for basic transcription factors in different tissues that express *DMPK* could account for the multisystemic and multisymptomic nature of DM1 findings (e.g., myotonia, myopathy, diabetes, testicular atrophy). Notably, the clinical analogies between DM1 and DM2, in which the latter has CCUG mRNA expansions (*25*), may conceivably derive from a common trans-acting mechanism with trapping and depletion of similar or identical TFs.

Other examples of transcriptional dysregulation in genetic disorders are the trichothiodystrophies, a group of autosomal recessive diseases (*26*), and Cockayne syndrome (*27*). All result from phenotype-specific mutations in genes encoding TFIIH, a multicomponent complex that has been implicated in transcription and DNA excision repair. Whereas repair defects explain the skin photosensitivity seen in a subset of patients, other disease phenotypes have been attributed to transcriptional defects (*26*). Deletion of the variable-number tandem-repeat structure that binds transcription repressor YY1 leads to transcriptional derepression in the respective chromosomal band, to result in facioscapulohumeral muscular dystrophy (*28*). This short list of genetic disorder transcription syndromes (*29*) can now perhaps be extended.

References and Notes

1. J. D. Brook *et al*., *Cell* **68**, 799 (1992).
2. G. Jansen *et al*., *Nature Genet.* **13**, 316 (1996).
3. A. D. Otten, S. J. Tapscott, *Proc. Natl. Acad. Sci. U.S.A.* **92**, 5465 (1995).
4. N. A. Timchenko *et al*., *J. Biol. Chem.* **276**, 7820 (2001).
5. A. V. Philips, L. T. Timchenko, T. A. Cooper, *Science* **280**, 737 (1998).
6. A. Mankodi *et al*., *Mol. Cell* **10**, 35 (2002).
7. N. Charlet-B et al, *Mol. Cell* **10**, 45 (2002).
8. R. P. Junghans, A. Ebralidze, B. Tiwari, *Neurogenetics* **3**, 59 (2001).
9. K. L. Taneja, M. McCurrach, M. Schalling, D. Housman, R. H. Singer, *J. Cell Biol.* **128**, 995 (1995).
10. B. M. Davis, M. E. McCurrach, K. L. Taneja, R. H. Singer, D. E. Housman, *Proc. Natl. Acad. Sci. U.S.A.* **94**, 7388 (1997).
11. Appropriate conditions for in vitro binding are insufficiently understood to replicate the selectivity of the TF binding process that occurs in vivo (Fig. 1). We observe only nonselective binding of purified TF in vitro with all RNAs, whether mutant RNA or heterologous unrelated RNAs (*12*). The same discordance can be inferred for conditions used for CUGBP binding in vitro (*31*) that fail to reproduce the selectivity for mutant versus wild-type RNA that is evident in vivo (*4*, *12*), (Fig. 1A).
12. A. Ebralidze *et al*., unpublished observations.
13. M. Nicolas, V. Noe, K. B. Jensen, C. J. Ciudad, *J. Biol. Chem.* **276**, 22126 (2001).
14. T. Kimura *et al*., *Neurosci. Lett.* **295**, 93 (2000).
15. GI: 479168 (*32*) with MatInspector V2.2 software (*33*).
16. M. E. Massari, C. Murre, *Mol. Cell. Biol.* **20**, 429 (2000).
17. Experimental details are available as supporting material on *Science* Online.
18. K. S. Rajavel, E. F. Neufeld, *Mol. Cell. Biol.* **21**, 5512 (2001).
19. Although mutant RNA double-strand hairpins of CUG-repeat domains have been noted in vitro by electron microscopy, and binding of CUGBP in vitro at their single-strand junctions (*31*), in vitro binding studies may be vulnerable to overinterpretation for the in vivo setting [compare note (*11*)]. In vivo mutant RNP extracted from cells has yet to be studied structurally in this fashion.
20. We apply the same standard of 30% change for "significantly" disturbed transcription as used in the HD study (*24*).
21. Seven additional genes were recently studied, of which three were significantly suppressed and four unchanged in mutant RNA–expressing cells. A total of nine genes have now been tested with TF "restorations." When Sp1 or Sp3 was overexpressed, full or partial recovery was seen in three out of four of the depressed genes, with the fourth presumably responding to depleted TFs not tested, by this model. In contrast, among the five genes that were unchanged in mutant RNA–expressing cells, none (0/5) was stimulated by TF overexpression.
22. A. W. Dunah *et al*., *Science* **296**, 2238 (2002).
23. R. N. Freiman, R. Tjian, *Science* **296**, 2149 (2002).
24. R. Luthi-Carter *et al*., *Hum. Mol. Genet.* **11**, 1911 (2002).
25. J. Finsterer, *Eur. J. Neurol.* **9**, 441 (2002).
26. E. Bergmann, J. M. Egly, *Trends Genet.* **17**, 279 (2001).
27. F. Le Page *et al*., *Cell* **101**, 159 (2000).
28. D. Gabellini, M. R. Green, R. Tupler, *Cell* **110**, 339 (2002).
29. W. Vermeulen *et al*., *Cold Spring Harb. Symp. Quant. Biol.* **59**, 317 (1994).
30. K. Ohshima, S. Kang, J. E. Larson, R. D. Wells, *J. Biol. Chem.* **271**, 16773 (1996).
31. S. Michalowski *et al*., *Nucleic Acids Res.* **27**, 3534 (1999).
32. C. Lorenz, C. Meyer-Kleine, K. Steinmeyer, M. C. Koch, T. J. Jentsch, *Hum. Mol. Genet.* **3**, 941 (1994).
33. K. Quandt, K. Frech, H. Karas, E. Wingender, T. Werner, *Nucleic Acids Res.* **23**, 4878 (1995).

34. We acknowledge the many collegial interactions with C. Thornton and T. Cooper, who supplied information, materials and advice that assisted many phases of the project. Supported by grants to R.P.J. from the Muscular Dystrophy Association and of the National Institute for Arthritis, Muscle, and Skin Diseases (NIAMS) of the NIH.

Supporting Online Material

www.sciencemag.org/cgi/content/full/1088679/DC1
SOM Text
Figs. S1 and S2
References and Notes

2 July 2003; accepted 19 November 2003
Published online 4 December 2003;
10.1126/science.1088679
Include this information when citing this paper.

Multiple Ebola Virus Transmission Events and Rapid Decline of Central African Wildlife

Eric M. Leroy,[1]* Pierre Rouquet,[2]† Pierre Formenty,[3]† Sandrine Souquière,[2] Annelisa Kilbourne,[4] Jean-Marc Froment,[5] Magdalena Bermejo,[5] Sheilag Smit,[6] William Karesh,[4] Robert Swanepoel,[6] Sherif R. Zaki,[7] Pierre E. Rollin[7]

Several human and animal Ebola outbreaks have occurred over the past 4 years in Gabon and the Republic of Congo. The human outbreaks consisted of multiple simultaneous epidemics caused by different viral strains, and each epidemic resulted from the handling of a distinct gorilla, chimpanzee, or duiker carcass. These animal populations declined markedly during human Ebola outbreaks, apparently as a result of Ebola infection. Recovered carcasses were infected by a variety of Ebola strains, suggesting that Ebola outbreaks in great apes result from multiple virus introductions from the natural host. Surveillance of animal mortality may help to predict and prevent human Ebola outbreaks.

Human Ebola virus (EBOV) infection causes hemorrhagic fever and death within a few days (*1*). The most lethal strains, causing up to 88% mortality, occur in Gabon, the Republic of Congo (RC), and the Democratic Republic of Congo (DRC) in central Africa, and belong to the Zaire subtype, which is one of four known EBOV subtypes. Together with Marburg virus, EBOV forms the *Filoviridae* family, a group of enveloped, nonsegmented, negative-strand RNA viruses (*2*). The genome is ~19,000 nucleotides long and bears linearly arranged genes that encode seven structural proteins and one nonstructural protein (*3*). Human Ebola outbreaks usually occur abruptly from an unidentified source, with subsequent spread from person to person (*4*). The first three known outbreaks of Ebola occurred between 1976 and 1979 in Zaire (now DRC) and Sudan, with 318 (*5*), 284 (*6*) and 34 (*7*) cases, respectively. No further cases were recognized in Africa until late 1994. Since then, EBOV has appeared in human beings eight times, in several sub-